



# Improved carbohydrate force field for GROMOS: ring and hydroxymethyl group conformations and exo-anomeric effect

Stéphane A.H. Spieser <sup>a,\*</sup>, J. Albert van Kuik <sup>b</sup>, Loes M.J. Kroon-Batenburg <sup>a</sup>,  
Jan Kroon <sup>a</sup>

<sup>a</sup> Department of Crystal and Structural Chemistry, Bijvoet Center for Biomolecular Research Utrecht University, Padualaan 8, NL-3584 CH Utrecht, The Netherlands

<sup>b</sup> Department of Bio-Organic Chemistry, Bijvoet Center for Biomolecular Research Utrecht University, Padualaan 8, NL-3584 CH Utrecht, The Netherlands

Received 19 April 1999; accepted 23 August 1999

## Abstract

In this work, improvements of the carbohydrate force field for GROMOS have been carried out by combined molecular mechanics (MM) and molecular dynamics (MD) calculations. With the original force field, a far too small relative energy (4.5 kJ mol<sup>-1</sup>) between the ‘normal’ chair conformation (<sup>4</sup>C<sub>1</sub>) and the ‘inverted chair’ conformation (<sup>1</sup>C<sub>4</sub>) of the methyl β-D-glucopyranoside has been observed in vacuum, compared with ab initio and MM3 calculations that predict 16.0–30.0 kJ mol<sup>-1</sup>. The ring inversion has been solved by a large increase of the bond-angle force constants involving the oxygen atom of hydroxyl groups. The consequence of such a modification for the relative energy between the two chair conformations is an increase to 13.2 kJ mol<sup>-1</sup>. Furthermore using a potential-of-mean-force calculation through umbrella sampling, with explicit solvent molecules, on both methyl β-D-glucopyranoside and methyl β-D-galactopyranoside, it has been found that the rotamer distribution of the hydroxymethyl group does not reproduce accurately NMR data. The hydroxymethyl group conformer distribution has been improved by increasing the torsional barrier around the considered bond (OA–CS2–CS1–OS) leading to a closer agreement with experimental rotamer distributions. In addition, an improved dihedral potential has been used to account for the exo-anomeric effect. MM calculations in vacuum on the methyl β-D-fructofuranoside have shown that our force field modifications have only a slight influence on the conformation of the five-membered ring. This was confirmed by MD simulation in aqueous solution. © 1999 Elsevier Science Ltd. All rights reserved.

**Keywords:** Carbohydrates; GROMOS; Force field; Ring conformation; Glucose; Fructose

## 1. Introduction

Three previous studies in our group have pointed out that there is a need for improvement of the sugar part of the GROMOS [1] force field [2] to better describe experimental

data. In the first one [3], it was found that the exocyclic two-fold O–C–C–O dihedral force constant in the GROMOS force field should be increased to better account for the gauche effect regarding the hydroxymethyl group in saccharides. The second one [4] showed that the exo-anomeric torsion angle  $\Phi$ , O–5–C–1–O–1–C–4 (see Fig. 1), was too often localised near 180° during molecular dynamics (MD)

\* Corresponding author. Tel.: +31-30-2533410/2532383; fax: +31-30-533940.

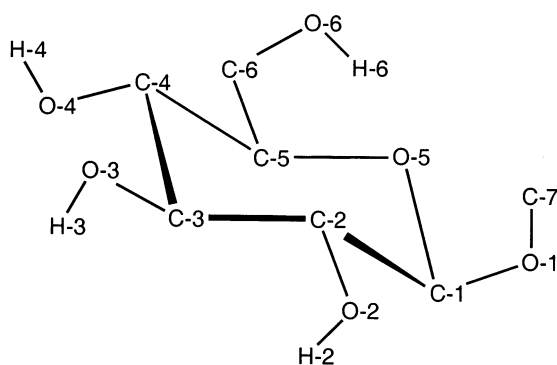


Fig. 1. Atom numbering in methyl  $\beta$ -D-glucopyranoside

simulations of methyl- $\beta$ -cellobioside in dimethyl sulfoxide. This is overcome by applying a specific two-fold dihedral potential on the exo-anomeric topology O–C–O–C. In the third one [5], it was observed that the unfavourable ‘inverted’ chair conformation, as well as boat conformations, occurred during long MD simulations of methyl- $\beta$ -cellobioside in water due to an underestimated bond angle potential (this paper). It is well established theoretically and experimentally that the glucopyranose rings preferentially adopt a chair over a boat conformation and specifically a conformation with all substituents in an equatorial position over the one with all substituents in an axial position. The goal of this work was to improve on these three aspects by modifying the GROMOS 87 force field. GROMOS 96 [6] is hardly different from GROMOS 87. Only the van der Waals parameters of the united atoms (atom types CS1 and CS2) are changed. The force field modifications that are described in this work would also be valid for GROMOS 96.

## 2. Methods

In this work we considered CH, CH<sub>2</sub> and CH<sub>3</sub> groups as united atoms, i.e., only with one interaction centre. The tetrahedral geometry of the carbon atoms was maintained using improper torsion potentials. All geometry optimisations used the steepest descent followed by conjugate gradient algorithms with a convergence criterion of  $1 \times 10^{-5}$  kJ mol<sup>-1</sup>. The notation *tg*; *gt*; *gg* for the conformation of the

hydroxymethyl groups will be used. For example *tg* means that O-6 is trans with respect to O-5 and gauche with respect to O-4. In the case of the fructose, the additional hydroxymethyl group is defined such that *tg* means that O-1 is trans with respect to O-5 and gauche with respect to O-2.

**Molecular mechanics on methyl  $\beta$ -D-glucopyranoside.**—Three sets of calculations in the isolated state were initiated either with the ‘normal’ <sup>4</sup>C<sub>1</sub> chair conformation, with the ‘inverted’ <sup>1</sup>C<sub>4</sub> chair conformation or with the <sup>3,05</sup>B boat conformation of the glucopyranose ring. The last has been chosen because of its occurrence during MD simulations. The starting structure of the <sup>4</sup>C<sub>1</sub> chair has been built by using crystal structure coordinates [7] present in the Cambridge Structural Database (CSD) data bank [8]. In the case of the <sup>1</sup>C<sub>4</sub> chair and the <sup>3,05</sup>B boat, atomic coordinates have been modified to arrive at the ‘perfect’ Cremer and Pople puckering parameters ( $\theta$ ,  $\phi$ ) [9]. Glucose has six freely rotatable groups where all torsional potentials have three local minima (staggered orientations). All  $3^6 = 729$  possible stereoisomers for each chair, or boat, were fully minimised.

**Potential-of-mean-force calculations and hydroxymethyl group rotamer distribution.**—In order to determine hydroxymethyl group rotamer distributions for  $\beta$ -D-glucopyranose and  $\beta$ -D-galactopyranose, potential-of-mean-force calculations were carried out in the same way as described previously [3]. Molecular dynamics simulations were performed on Silicon Graphics O2 computers. Each monosaccharide was surrounded by 266 SPC/E [10] water molecules in a truncated octahedron with periodic boundary conditions. All bond lengths were kept fixed using the SHAKE procedure [11]. The cut-off radius was 8 Å and a time step of 2 fs was used. Simulations were performed with loose coupling to a pressure bath at 1 atm and a temperature bath at 300 K [12] with time constants of 0.5 and 0.1 ps, respectively.

All simulations took 2 ns and were divided into jobs of 10 ps. The  $\phi$  values were collected into 72 five-degree bins. The derivatives were fitted to a 12-term Fourier series by the least-squares singular value decomposition al-

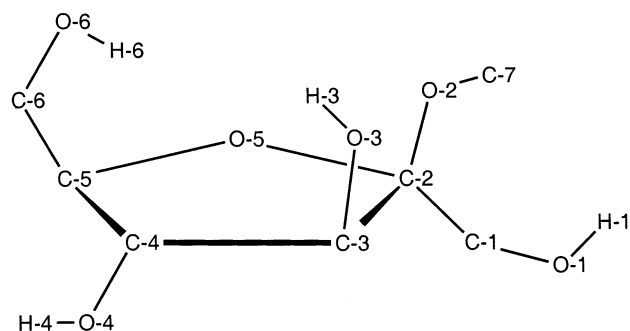


Fig. 2. Atom numbering in methyl  $\beta$ -D-fructofuranoside.

gorithm [13]. The first 0.2 ps of each job were discarded. Integration gave the potential of mean force ( $\Delta G$ ).

Hypothetical NMR coupling constants were computed from the dihedral torsion angles H-5–C-5–C-6–H-6<sub>proR</sub> and H-5–C-5–C-6–H-6<sub>proS</sub> (aliphatic H-atoms are calculated at idealised positions) for each of the 72 bins with the formulae of Haasnoot et al. [14] and coupling constants  $^3J_{5,6\text{proR}}$  and  $^3J_{5,6\text{proS}}$  were calculated for both D-glucose and D-galactose as a weighted average of those.

**Molecular mechanics on methyl  $\beta$ -D-fructofuranoside.**—Two sets of calculations in the isolated state were initiated either with the  $^3E$  envelope conformation or the  $^4E$  envelope conformation. The starting structures were built by using crystal structure coordinates

[15] present in the CSD of disaccharides or trisaccharides containing a fructofuranose residue. Fructose has seven rotating groups; all  $3^7 = 2187$  possible stereoisomers for each envelop conformation were fully minimised (Fig. 2).

**Molecular dynamics on methyl  $\beta$ -D-fructofuranoside.**—The minimum-energy conformer of the methyl  $\beta$ -D-fructofuranoside was surrounded by 127 SPC/E water molecules in a truncated octahedron with periodic boundary conditions. All bond lengths were kept fixed using the SHAKE procedure. The cut-off radius was 8 Å and a time step of 2 fs was used. Simulations were performed with loose coupling to a pressure bath at 1 atm and a temperature bath at 300 K with time constants of 0.5 and 0.1 ps, respectively. The simulation took 500 ps.

### 3. Results and discussion

**Methyl  $\beta$ -D-glucopyranoside.**—All 729 potential stereoisomers for each chair led after optimization to 62 unique  $^4C_1$  chairs and 52 unique  $^1C_4$  chairs. One conformer was defined as not stationary on the hypersurface if its Cartesian coordinates had a rms deviation with a lower energy structure smaller than

Table 1

Energy (kJ mol<sup>−1</sup>) comparisons between the three ring conformations of the methyl  $\beta$ -D-glucopyranoside, using the original (INI) and the modified (NEW) GROMOS force fields

Energy terms <sup>a</sup>	$\beta$ -D-Glucoside (INI)			$\beta$ -D-Glucoside (NEW)		
	$^1C_4$	$^4C_1$	$^{3,5}B$	$^1C_4$	$^4C_1$	$^{3,5}B$
$E_T$	269.5	265.0	287.2	288.6	275.4	298.3
$\Delta E$	+4.5	0.0	+22.2	+13.2	0.0	+22.9
$E_{ES}$	210.1	227.5	223.1	214.5	232.7	228.3
$E_{vdW}$	5.2	5.1	5.8	5.1	4.8	7.0
$E_{bH}$	1.7	0.9	1.3	1.7	0.9	1.3
$E_{bnH}$	4.9	2.9	4.3	5.3	3.0	4.8
$E_{aH}$	0.6	1.7	0.2	0.5	1.6	0.2
$E_{anH}$	12.6	2.5	5.4	25.1	4.2	8.9
$E_{ImpDih}$	4.0	0.3	1.1	3.0	0.2	0.2
$E_{DihH}$	2.8	2.0	6.4	3.2	1.7	6.3
$E_{DihnH}$	27.5	22.1	39.4	30.1	26.3	41.1

<sup>a</sup>  $E_T$  is the total energy;  $\Delta E$  is the relative energy;  $E_{ES}$  is the electrostatic energy term;  $E_{vdW}$  is the van der Waals energy term;  $E_{bH}$  is the bond energy term with H atoms;  $E_{bnH}$  is the bond energy term without H atoms;  $E_{aH}$  is the bond angle energy term with H atoms;  $E_{anH}$  is the bond angle energy term without H atoms;  $E_{ImpDih}$  is the improper dihedral energy term;  $E_{DihH}$  is the dihedral energy term with H atoms and  $E_{DihnH}$  is the dihedral energy term without H atoms.

0.05 Å. The global minimum-energy conformer (Table 1) obtained by the original GROMOS force field has a ‘normal’ chair conformation, with an energy  $4.5 \text{ kJ mol}^{-1}$  lower than the ‘inverted’ chair conformation. From *ab initio* calculations, as well as other molecular mechanics (MM) calculations [16,17], an energy difference of  $16.0\text{--}30.0 \text{ kJ mol}^{-1}$ , in favour of the ‘normal’ chair conformation, is expected. Indeed, the ‘inverted’ chair conformation presents all substituents of the aldopyranose ring in an axial position. This conformational arrangement induces highly unfavourable steric interactions, commonly referred to as the 1,3 syn-diaxial interactions.

Table 1 shows the values for each energy term. No energy differences in the van der Waals term between the two chair forms are noticeable. The angle bending term involving non-hydrogen atoms tends to destabilize, ca  $10 \text{ kJ mol}^{-1}$ , the ‘inverted’ chair conformation, but this is far too little to compensate the electrostatic stabilisation, ca  $17 \text{ kJ mol}^{-1}$ , which was due to shorter hydrogen bonds (same result as Barrows et al. [17]). In the same way, the improper dihedral and the dihedral potentials show a slight destabilization ( $3.7$  and  $5.4 \text{ kJ mol}^{-1}$ , respectively) of the ‘inverted’ chair. Altogether, an energy difference between the two chair conformations of the order of  $4.5 \text{ kJ mol}^{-1}$  is far too small, and might be a main reason for the occurrence of the ‘inverted’ chair conformation in MD simulations.

For the boat conformation, 72 unique conformers were found. As expected, a high energy is calculated due to the two eclipsed ring torsions. The torsional term correctly describes this. Here also the van der Waals term is only a bit higher than the ‘normal’ chair conformation.

In Table 2, the original GROMOS force field predicts a ‘normal’ chair conformation with a puckering amplitude in good agreement with the crystal structure or quantum mechanics calculations [16,17]. The puckering parameter  $\theta$  even shows that the  $^4C_1$  chair stays very close to a ‘perfect’ chair form. The hydroxymethyl group has a *tg* orientation. According to experimental NMR results [18,19], the occurrence of such a rotamer is low. Its energy

must thus be larger than for the *gt* and *gg* conformations due to the so-called gauche effect. The opposite result observed here is a consequence of the isolated-state calculation, which tends to maximise intramolecular hydrogen bonds. The secondary hydroxyl groups present a counterclockwise orientation with weak intramolecular hydrogen bonds. Nevertheless the bond and torsion angles of the pyranose ring are in satisfactory agreement with experimental crystal structure [7], and previous calculations [17].

Both ‘inverted’ chair and boat conformations are slightly distorted. Some bond angles in the ‘inverted’ chair conformation, specifically those involving the oxygen atoms of hydroxyl groups, showed deviations up to  $7^\circ$  with respect to equilibrium values. Such deviations resulted in a more remote position of two diaxial hydroxyl groups, in order to avoid unfavourable steric interactions. However, the bond angle energy increased only moderately (ca  $10.0 \text{ kJ mol}^{-1}$ ). Ott and Meyer [20] already mentioned the necessity to adjust the bond angle term, but did not do so. Both ‘inverted’ chair and ‘normal’ chair minimum energy structures were also optimised with the MM3(92) force field [21] (dielectric constant 1.5). No such large deviations in the bond angle geometries occurred with MM3(92). Thus, we have decided to increase all bond angle force constants and to change some bond angle equilibrium values, listed in Table 3, using MM3 geometries as a guide.

At the same time, two new dihedral potentials have been introduced. The first one, OA–CS2–CS1–OS, is changed according to Ref. [3], to better reproduce the experimental distribution of the hydroxymethyl group. The second one, OS–CS1–OSE–CS1, as described in Ref. [4], is added to simulate the exo-anomeric effect, and to avoid the trans conformation of an exo-cyclic substituent at the anomeric centre. A new atom type OSE has been created to distinguish the endo-anomeric effect from the exo-anomeric effect. This new atom type is identical in all points to the OS atom type except for the CS1–OSE–CS1 bond angle and the X–CS1–OSE–X dihedral potential (where X means any atom type). Using the same dihedral potential for the endo-anomeric

Table 2

Comparisons of global minimum geometries for each of the three ring conformations of the methyl  $\beta$ -D-glucopyranoside with both original (INI) and modified GROMOS (NEW) force fields

	$\beta$ -D-Glucoside INI			$\beta$ -D-Glucoside NEW			$\beta$ -D-Glucoside crystal
	${}^1C_4$	${}^4C_1$	${}^{3,05}B$	${}^1C_4$	${}^4C_1$	${}^{3,05}B$	${}^4C_1$
<i>Ring puckering</i>							
$q$ (Å)	0.519	0.597	0.708	0.482	0.615	0.715	0.594
$\theta$ (°)	167.8	0.6	95.5	170.5	2.3	90.7	6.5
$\phi$ (°)	347.0	<sup>a</sup>	11.9	340.5	<sup>a</sup>	13.7	<sup>a</sup>
<i>Bond angles</i> (°)							
C-1-O-1-C-7	111.1	111.4	111.5	110.5	112.0	112.1	113.4
O-1-C-1-C-2	114.8	109.1	109.2	111.5	108.1	108.2	109.6
O-1-C-1-O-5	106.9	109.2	110.7	108.1	107.5	108.4	108.3
O-2-C-2-C-1	112.5	113.6	111.3	109.8	111.2	109.0	111.1
O-2-C-2-C-3	109.1	110.3	109.4	107.3	108.4	107.1	109.3
O-3-C-3-C-2	114.4	110.3	112.7	112.0	108.8	110.0	107.9
O-3-C-3-C-4	112.2	109.9	111.6	110.5	108.9	109.6	110.4
O-4-C-4-C-3	110.1	109.5	109.5	107.9	107.7	107.7	109.3
O-4-C-4-C-5	110.0	112.7	110.7	108.1	110.4	108.6	108.5
C-6-C-5-C-4	116.0	110.8	109.5	116.0	110.8	110.4	112.5
C-6-C-5-O-5	113.1	109.5	108.2	112.3	108.1	107.4	107.1
O-6-C-6-C-5	114.9	110.2	113.4	112.3	107.7	110.5	113.3
O-5-C-1-C-2	113.0	110.3	114.2	112.8	108.1	111.4	108.6
C-1-C-2-C-3	109.9	107.3	111.2	111.9	108.1	112.4	108.4
C-2-C-3-C-4	110.3	111.7	109.5	111.6	110.5	110.7	110.7
C-3-C-4-C-5	112.1	108.1	109.9	113.4	108.8	111.2	111.4
C-4-C-5-O-5	112.3	110.0	114.7	112.8	108.5	112.9	108.4
C-5-O-5-C-1	119.0	112.7	114.5	119.4	112.4	113.8	111.8
<i>Dihedral angles</i> (°)							
C-7-O-1-C-1-O-5	-153.6	-71.8	-69.0	-88.5	-77.3	-76.5	-72.4
H-2-O-2-C-2-C-1	-88.8	56.9	108.8	32.7	59.6	124.8	89.4
O-2-C-2-C-1-O-5	70.4	179.9	129.4	70.0	178.5	132.7	-178.8
O-2-C-2-C-1-O-1	-166.7	-60.1	-105.9	-168.1	-65.3	-108.2	-60.6
H-3-O-3-C-3-C-2	90.3	-40.8	107.3	91.2	-44.3	105.7	173.0
O-3-C-3-C-2-O-2	165.1	56.4	160.0	167.2	62.6	161.1	63.6
H-4-O-4-C-4-C-3	158.7	40.9	-22.6	154.8	44.3	-23.2	101.0
O-4-C-4-C-3-O-3	-164.0	-57.4	-173.2	-165.5	-64.4	-175.8	-68.8
H-6-O-6-C-6-C-5	63.1	35.3	173.0	63.1	35.5	174.0	-56.9
O-6-C-6-C-5-O-5	-66.1	176.8	-66.9	-69.6	176.3	-67.8	68.0
O-5-C-1-C-2-C-3	-51.4	57.7	7.2	-49.0	59.6	14.1	61.1
C-1-C-2-C-3-C-4	56.5	-56.8	48.2	52.2	-57.2	42.1	-54.3
C-2-C-3-C-4-C-5	-55.6	56.8	-60.5	-50.6	56.5	-56.2	51.9
C-3-C-4-C-5-O-5	47.7	-56.9	16.5	44.8	-57.9	12.7	-54.2
C-4-C-5-O-5-C-1	-44.4	61.5	40.4	-43.7	64.2	46.7	62.8
C-5-O-5-C-1-C-2	46.8	-62.2	-53.5	46.0	-65.2	-61.3	-67.3

<sup>a</sup> Small values for  $\theta$  make comparison of  $\phi$  pointless.

effect affects the ring conformations in an unfavourable way. It would demand the reoptimisation of all ring dihedral parameters. The development of a new force field is outside the scope of this paper and only minimal corrections to GROMOS are sought.

Table 1 shows that the ‘normal’ chair conformation is now favoured by ca 13 kJ mol<sup>-1</sup>. Nevertheless a larger energy difference should still be expected. The bond angle energy of the

‘inverted’ chair minimum, increases a lot, up to twice the previous amount. At the same time the ‘normal’ chair conformation experiences only a minor increase of this energy. The situation of the dihedral angle term, involving no hydrogen atoms, is more complex. First, the hydroxymethyl group in the ‘normal’ chair minimum is located in a trans orientation, which is an artefact of the isolated state calculation (vide supra). Secondly all

endo-cyclic O–C–C–O torsion angles with a trans orientations (three) in the ‘inverted’ chair conformation (average value 165°) deviate from the ideal position (180°), while those (two) in the ‘normal’ chair conformation (average value 176°) are located close to this ideal value. Therefore the destabilisation expected from the torsional barrier, for the ‘inverted’ chair, tends to vanish.

The puckering parameters of the ‘normal’ chair conformation (Table 2) are only slightly affected by the force field modifications. Its general geometry shows an even better agreement with experimental crystal structure. Both ‘inverted’ chair and boat conformations are less distorted as depicted by the puckering parameters. The deviations of bond angles in the ‘inverted’ chair conformation are still present but are less and at a higher energy cost. The boat conformation experiences no real changes, keeping a high energy compared with the ‘normal’ chair conformation.

Two 10 ns MD simulations in water of methyl  $\beta$ -cellobioside (to be published), using this modified force field, show that the ‘inverted’ chair conformation no longer oc-

curred. Nevertheless boat conformations still appear from time to time (less than 3% of the simulation time), showing that the ring keeps some flexibility.

*Potential-of-mean-force calculations and the hydroxymethyl group rotamer distribution.*—In order to study the behaviour of the hydroxymethyl group with the new bond angle force constants, and with the enhanced OA–CS2–CS1–OS dihedral term, potential-of-mean-force calculations were run with the GRO-MOS force field for  $\beta$ -D-glucopyranose and  $\beta$ -D-galactopyranose. These calculations show the free energy differences of three conformations, *gg*, *gt* and *tg*. The calculations were performed with the original GROMOS force field (INI), a modified force field that contains only the bond angle changes (INI+), and the fully modified force field (NEW). Probability distributions (Fig. 3) were calculated from the free energies and compared with abundances from crystal structure data acquired from the CSD (Table 4). An alternative method to judge the quality of the calculated distributions is by comparing calculated and experimental  $^3J$  NMR coupling constants.

Table 3  
Detailed force field parameter modifications

	Force constants (kcal mol <sup>-1</sup> rad <sup>-2</sup> )		Equilibrium values (°)		
	INI	NEW	INI	NEW	
<i>Bond angle term</i>					
CS1–OS–CS1	80.0	110.0	109.5	<sup>a</sup>	
CS1–CS1–O <sup>b</sup>	68.0	110.0	109.5	107.0	
CS1–CS1–CS1	60.0	110.0	109.5	<sup>a</sup>	
CS2–CS1–OS	68.0	110.0	109.5	107.0	
CS2–CS1–CS1	60.0	110.0	109.5	<sup>a</sup>	
CS1–CS2–OA	68.0	110.0	109.5	107.0	
OS–CS1–OS	80.0	110.0	109.5	107.0	
CS1–OSE <sup>c</sup> –CS1		80		111 <sup>d</sup>	
	Force constants (kcal mol <sup>-1</sup> )		Multiplicity <i>n</i>	Phase angle $\delta$ (°)	
<i>Dihedral term</i>					
OS–CS1–OSE <sup>c</sup> –CS1		1.0	2	0	exo-anomeric effect
OA–CS2–CS1–OS	0.5	1.0	2	0	gauche effect

<sup>a</sup> Unchanged.

<sup>b</sup> OA as well as OS.

<sup>c</sup> Atom type OSE equivalent to OS for all other parameters.

<sup>d</sup> Bond angle equilibrium value was chosen by comparing the average C-1–O-1–C-4 angle in MD simulations of methyl- $\beta$ -cellobioside in water with the average glycosidic bond angle of disaccharides in crystal structure.

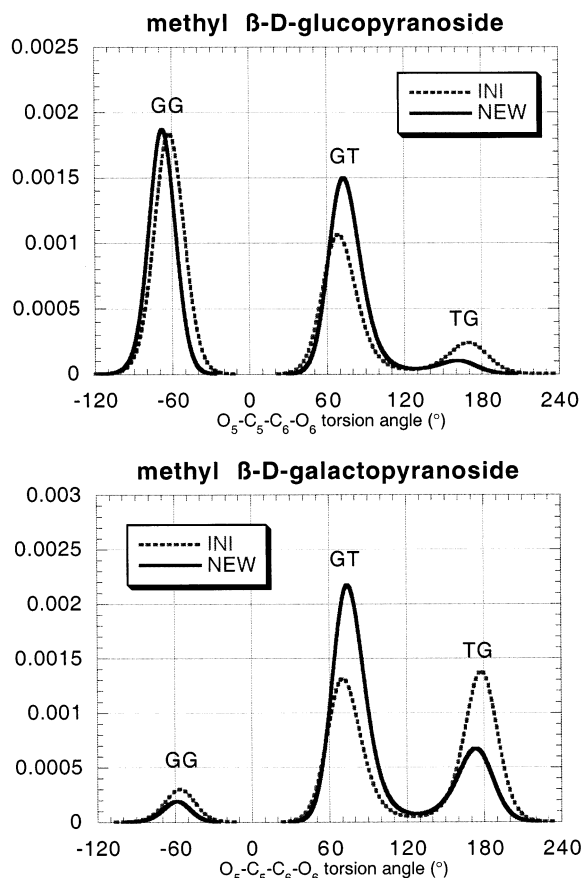


Fig. 3. Probability distribution profiles of the hydroxymethyl orientation in methyl  $\beta$ -D-glucopyranoside and methyl  $\beta$ -D-galactopyranoside with the original (INI) and modified (NEW) force field obtained by potential-of-mean-force calculations in water. Each point represents the integrated probability density over a  $5^\circ$  bin.

Experimental, as well as the calculated NMR coupling constants  $^3J_{5,6\text{pro}R}$  and  $^3J_{5,6\text{pro}S}$ , for both  $\beta$ -D-glucopyranose and  $\beta$ -D-galactopyran-

ose are also presented in Table 4. One important criterion for the improvement of the modified force field is how well it reproduces the low occurrence of the *tg* conformation of  $\beta$ -D-glucose, which was far too abundant in the original force field. The completely modified GROMOS force field gives a profound reduction of this distribution, while a change of only the bond angle terms has no significant effect. The coupling constants derived from the original GROMOS force field are clearly not acceptable. Both modified force fields do a little better. For  $\beta$ -D-galactose, the *gt* conformation is the distinct favourite, a feature that is only reflected by the fully modified GROMOS force field. This force field is also the only one to produce reliable coupling constants.

**Methyl  $\beta$ -D-fructofuranoside.**—It has been pointed out by Olson [22] that using large bond angle force constants leads to a description of furanose geometries in considerable disagreement with solid state examples [23]. These five-membered ring molecules are known to be highly flexible [24]. However, from the work of French et al. [25,26], two or three conformations of the furanic ring are mostly expected ( $^3E$ ,  $^4_3T$  and  $^4E$ ). We have studied both  $^3E$  ( $\phi = 255^\circ$ ) and  $^4E$  ( $\phi = 285^\circ$ ) conformers, because they are located within 4 kJ mol $^{-1}$  of the energy minimum (ring puckering parameter  $\phi$  in the range  $240$ – $290^\circ$ ), where most of the crystal structures are also found.

Table 4

Probability distributions of conformations of the  $\beta$ -D-glucoside and  $\beta$ -D-galactoside hydroxymethyl-group, and derived NMR coupling constants, using the original and modified GROMOS force fields

Distribution	$\beta$ -D-Glucoside				$\beta$ -D-Galactoside			
	INI	INI+ <sup>a</sup>	NEW	CSD <sup>b</sup>	INI	INI+ <sup>a</sup>	NEW	CSD <sup>b</sup>
<i>gg</i>	54	40	48	56	9	4	5	7
<i>gt</i>	36	48	47	43	44	44	70	61
<i>tg</i>	10	12	5	1	47	52	25	32
$^3J$				NMR <sup>c</sup>				NMR <sup>c</sup>
$J_{5,6\text{pro}R}$	4.4	5.5	5.2	6.0	6.5	6.4	7.3	7.7
$J_{5,6\text{pro}S}$	3.2	3.1	2.3	2.2	6.2	6.5	4.1	4.4

<sup>a</sup> INI+ includes only the bond angle changes.

<sup>b</sup> Values were taken from Ref. [3].

<sup>c</sup> Measured at 500 MHz and 300 K. Values were determined by simulation of the spectra.

Table 5

Energy (kJ mol<sup>-1</sup>) terms of the methyl  $\beta$ -D-fructofuranoside conformations using the original (INI) and the modified (INI+, NEW) GROMOS force fields

Energy terms <sup>a</sup>	$\beta$ -D-Fructoside INI		$\beta$ -D-Fructoside INI+		$\beta$ -D-Fructoside NEW	
	${}_3E$	${}_4E$	${}_3E$	${}_4E$	${}_3E$	${}_4E$
$E_T$	349.8	349.8	375.7	375.7	384.9	384.9
$E_{ES}$	281.7	281.6	296.1	295.6	303.6	303.5
$E_{vdW}$	-7.0	-7.0	-7.4	-7.3	-7.3	-7.3
$E_{bH}$	0.8	0.8	0.7	0.7	0.4	0.4
$E_{bnH}$	3.4	3.4	4.3	4.3	4.9	4.9
$E_{aH}$	0.9	0.9	0.7	0.7	0.4	0.4
$E_{anH}$	25.7	26.0	33.6	34.0	29.4	29.5
$E_{ImpTor}$	0.8	0.8	1.2	1.3	0.7	0.7
$E_{TorH}$	3.0	3.0	2.8	2.9	1.8	1.8
$E_{TornH}$	40.4	40.2	43.6	43.5	51.1	51.0

<sup>a</sup> See Table 1 for legend.

Table 5 presents the total energy value and the values for each term of the potential energy function. From the two starting ring conformations, energy minimisations of the 2187 conformers, using the original GROMOS force field, led to 374 unique structures starting from a  ${}_3E$  ring conformation and 456 unique structures starting from a  ${}_4E$  ring conformation. The minimum energy structures obtained from both starting ring conformation had the same total energy as well as equivalent term-by-term energy values. It appears that a unique conformation is reached. This is confirmed in Table 6 by the puckering parameters, which are similar. Comparison with the global minimum reported by French et al. [26], using MM3, shows a good agreement for the phase puckering parameter, but the ring appears to be more puckered. Geometrical parameters (Table 6) show a reasonable agreement with MM3. However, here again, the bond angles involving the oxygen atoms of hydroxyl groups present large values with respect to the MM3 minimum. Moreover, both hydroxymethyl groups are located in *tg* orientation, which allows a weak intramolecular cyclic hydrogen bond network to occur, while MM3 predicts the two hydroxymethyl groups in *gt* and *gg* conformation for C-6 and C-1, respectively.

Using our modified force field leads to an equivalent result as with the original one, i.e., energy terms and ring puckering parameters

show that a unique conformer is reached starting from both initial ring conformations. While the puckering amplitude tends to be in much closer agreement with the MM3 calculations or crystal structure average, the phase parameter experiences a shift, from 255° ( ${}_3E$ ) or 285° ( ${}_4E$ ), to 240° ( ${}_2T$ ). This locates our minimum at the edge of the energy minimum area 6.3 kJ mol<sup>-1</sup> above the minimum described by French et al. As Table 6 shows, bond angle values are now smaller and in better agreement with MM3 and one hydroxymethyl group C-5 adopts a gauche conformation (*gt*). The immediate effect is to break the intramolecular hydrogen bond network, which was present using the original force field, and to create a strong O-6–H-6···O-2. This could explain the change of the puckering phase, because this hydrogen bond forces the C-2 carbon atom out of the plane of the ring.

Tables 5 and 6 also present calculations with a modified force field involving only the bond angle change (INI+), without the gauche effect potential. This shows that again a unique conformer is reached for both ring starting structures. But the agreement with MM3 is quite good both for the puckering and the geometrical parameters. So on one hand, it seems that drastically increasing the bond angle force constants does not have a large effect on the ring conformation, but on the other hand, the addition of the gauche



Table 6

Comparison of selected geometries of methyl  $\beta$ -D-fructofuranoside using the original (INI), only bond angle term modifications (INI+) and modified (NEW) force fields <sup>a</sup>

	$\beta$ -D-Fructoside INI		$\beta$ -D-Fructoside INI +		$\beta$ -D-Fructoside NEW		$\beta$ -D-Fructoside	
	${}_3E \rightarrow {}_3T$	${}_4E \rightarrow {}_3T$	${}_3E \rightarrow {}_3T$	${}_4E \rightarrow {}_3T$	${}_3E \rightarrow {}_3T$	${}_4E \rightarrow {}_3T$	MM3	crystal <sup>(a)</sup>
<i>Ring puckering</i>								
<i>q</i>	0.478	0.481	0.449	0.452	0.386	0.387	0.404	0.352
<i><math>\phi</math></i>	264.0	264.7	259.4	261.0	240.5	240.7	260.8	252.0
<i>Bond angles (°)</i>								
O-2-C-2-O-5	107.6	107.6	109.3	109.3	106.8	106.8	108.0	111.1
O-2-C-2-C-3	110.8	110.8	110.0	110.0	111.2	111.2	108.4	104.8
O-2-C-2-C-1	115.5	115.5	113.5	113.5	115.0	115.0	110.1	111.2
O-1-C-1-C-2	114.2	114.2	110.5	110.5	111.4	111.4	108.9	113.3
C-1-C-2-O-5	113.6	113.6	112.2	112.2	111.6	111.7	110.9	108.2
C-1-C-2-C-3	104.8	104.8	108.2	108.2	109.0	109.0	113.4	116.8
O-3-C-3-C-2	118.4	118.4	115.5	115.5	114.6	114.6	111.8	113.5
O-3-C-3-C-4	116.3	116.3	113.4	113.5	112.5	112.6	111.1	115.2
O-4-C-4-C-3	114.8	114.8	111.2	111.2	108.7	108.7	110.1	113.3
O-4-C-4-C-5	113.8	113.9	111.2	111.2	111.3	111.3	110.0	110.1
C-6-C-5-C-4	110.2	110.4	110.4	110.5	111.1	111.1	113.1	113.6
C-6-C-5-O-5	113.9	114.0	111.4	111.5	110.6	110.6	108.9	111.1
O-6-C-6-C-5	111.1	111.1	108.1	108.0	110.4	110.4	109.8	109.3
O-5-C-2-C-3	103.8	103.8	102.9	103.0	102.4	102.4	105.8	104.5
C-2-C-3-C-4	99.4	99.4	100.6	100.6	103.0	103.0	101.1	102.3
C-3-C-4-C-5	99.0	98.9	100.7	100.5	102.9	102.8	101.2	103.2
C-4-C-5-O-5	106.5	106.4	105.9	105.9	106.9	106.9	106.6	106.4
C-5-O-5-C-2	107.3	107.3	108.4	108.4	108.7	108.7	108.2	110.5
<i>Dihedral angles (°)</i>								
C-7-O-2-C-2-O-5	-64.2	-64.2	-60.5	-60.4	-69.5	-69.5	-65.6	-55.8
H-1-O-1-C-1-C-2	25.8	25.7	19.4	19.1	-175.5	-175.5	-177.6	-89.8
O-1-C-1-C-2-O-2	65.1	65.0	65.6	65.7	71.2	71.3	-56.1	-179.9
O-1-C-1-C-2-O-5	-169.9	-169.9	-169.7	-169.7	-166.9	-166.8	63.5	-57.5
H-3-O-3-C-3-C-2	155.0	155.4	158.6	158.3	-45.1	-45.2	34.9	30.5
O-3-C-3-C-2-O-2	-54.2	-54.2	-47.9	-47.6	-48.9	-49.0	-40.4	-42.7
O-3-C-3-C-2-O-5	-169.4	-169.4	-164.4	-164.1	-162.7	-162.8	-156.1	-159.7
H-4-O-4-C-4-C-3	-159.3	-158.9	-163.3	-162.5	63.6	63.6	69.9	99.7
O-4-C-4-C-3-O-3	-63.2	-62.9	-73.7	-73.3	-83.8	-83.6	-85.2	-83.7
H-6-O-6-C-6-C-5	-173.0	-171.8	-173.5	-173.1	28.9	28.8	-61.4	134.0
O-6-C-6-C-5-O-5	-178.0	-178.3	-179.4	-179.4	-67.6	-67.5	67.4	66.2
O-5-C-2-C-3-C-4	-42.6	-42.4	-41.9	-41.5	-40.1	-40.2	-37.8	-34.9
C-2-C-3-C-4-C-5	46.9	47.2	44.4	44.8	34.1	34.3	39.7	33.6
C-3-C-4-C-5-O-5	-36.6	-37.2	-31.8	-32.9	-16.2	-16.4	-29.2	-21.2
C-4-C-5-O-5-C-2	10.3	11.1	5.7	7.1	-9.3	-9.1	6.0	-0.9
C-5-O-5-C-2-C-3	20.1	19.6	22.5	21.4	30.5	30.5	20.0	22.6

<sup>a</sup> Average over fructofuranose residues in disaccharide molecules found in the CSD.

effect affects the intramolecular hydrogen bond system, and the very flexible five-membered ring undergoes conformational transitions due to these weak intramolecular hydrogen bonds.

By MD simulations on the minimum-energy conformer of methyl  $\beta$ -D-fructofuranoside with explicit water molecules, the relevance of intramolecular hydrogen bonds can be assessed. The analysis of the distribution of the puckering parameter,  $\phi$ , with respect of

the puckering amplitude shows that the five-membered ring explores the whole low-energy area defined by French et al. The average value is  $\phi = 267^\circ$  and both hydromethyl groups adopt a gauche conformation. After 15 ps, no more intra molecular hydrogen bonds are observed. For a few ps, a transition to the low-energy region is even observed. Here again, the large increase of the bond angle force constants does not restrain the flexibility of the ring.

## 4. Conclusions

The original GROMOS force field has proved to be reliable for the modelling of hydrogen bonds in carbohydrates in water [27,28]. In this paper we have underlined that the original force field underestimates the energy cost of 1,3 syn-diaxial interactions. Weak bond angle force constants allow conformations with such arrangements to be present in the ensemble of low-energy minima. We have shown that increasing these force constants allows us to strongly stabilise the ‘normal’ chair conformations of glucopyranose rings without distorting their geometries. Moreover, the modification in the bond angle potential has a relatively small influence on the fructofuranose ring. However, slight changes in the geometries of furanose rings are observed due to the use of the extra gauche effect recommended by Klewinghaus et al. [3], but are mainly due to isolated state calculations with the concomitant influence of intramolecular hydrogen bonds. This has been demonstrated by MD simulation with explicit water molecules.

## Acknowledgements

This work was supported by The Netherlands Program for Economic Ecology and Technology, # EETK96095, and with financial aid from the Ministry of Economic Affairs and the Ministry of Education, Culture and Sciences.

## References

- [1] W.F. van Gunsteren, H.J.C. Berendsen, GROMOS-87 : Groningen Molecular Simulation Program Package. University of Groningen, The Netherlands, Groningen, 1987.
- [2] J.E.H. Koehler, W. Saenger, W.F. van Gunsteren, *Eur. Biophys. J.*, 15 (1987) 197–210.
- [3] P. Klewinghaus, B.P. van Eijck, M.L.C.E. Kouwijzer, J. Kroon, *J. Mol. Struct. (Theochem)*, 395–396 (1997) 289–295.
- [4] P.H. Kruiskamp, *PhD thesis*, University of Utrecht, 1998.
- [5] L.M.J. Kroon-Batenburg, P.H. Kruiskamp, J.F.G. Vliegthart, J. Kroon, *J. Phys. Chem. B*, 101 (1997) 8454–8459.
- [6] W.F. van Gunsteren, S.R. Billeter, A.A. Eising, P.H. Hünenberger, A.E. Mark, W.R.P. Scott, I.G. Tironi, *Biomolecular Simulation: The GROMOS-96 Manual and User Guide*. Hochschulverlag AG an der ETH Zürich and BIOMOS b.v., Zürich, Groningen, 1996.
- [7] S.S.C. Chu, G.A. Jeffrey, *Acta Cryst.*, B24 (1968) 830–838.
- [8] F.H. Allen, O. Kennard, *Chem. Design. Automation News*, 8 (1993) 31–37.
- [9] D. Cremer, J.A. Pople, *J. Am. Chem. Soc.*, 97 (1975) 1354–1358.
- [10] H.J.C. Berendsen, J.R. Grigera, T.P. Straatsma, *J. Phys. Chem.*, 91 (1987) 6269–6271.
- [11] J.P. Ryckaert, G. Ciccotti, H.J.C. Berendsen, *J. Comp. Phys.*, 23 (1977) 327–341.
- [12] H.J.C. Berendsen, J.P.M. Postma, W.F.v. Gunsteren, A. DiNiola, J.R. Haak, *J. Chem. Phys.*, 81 (1984) 3684–3690.
- [13] W.H. Press, B.P. Flannery, S.A. Teukolsky, W.T. Vetterling, *Numerical Recipes*, Cambridge University Press, Cambridge, 1989.
- [14] C.A.G. Haasnoot, F.A.A.M.d. Leeuw, C. Altona, *Tetrahedron*, 36 (1980) 2783–2792.
- [15] (a) T. Taga, E. Inagaki, Y. Fujimori, S. Nakamura, *Carbohydr. Res.*, 251 (1994) 203–212. (b) G.M. Brown, H.A. Levy, *Acta Crystallogr.*, B29 (1973) 790–794.
- [16] G.I. Csonka, K. Elias, I.G. Csizmadia, *Chem. Phys. Lett.*, 257 (1996) 49–60.
- [17] S.E. Barrows, F.J. Dulles, C.J. Cramer, A.D. French, D.G. Truhar, *Carbohydr. Res.*, 276 (1995) 219–251.
- [18] Y. Nishida, H. Ohrui, H. Meguro, *Tetrahedron Lett.*, 25 (1984) 1575–1578.
- [19] B.R. Leeftang, *PhD thesis*, Utrecht University, 1991.
- [20] K.-H. Ott, B. Meyer, *J. Comp. Chem.*, 17 (1996) 1068–1084.
- [21] N.L. Allinger, X. Zhou, J. Bergsma, *J. Mol. Struct. (Theochem)*, 312 (1994) 69–83.
- [22] W.K. Olson, *J. Am. Chem. Soc.*, 104 (1982) 278–286.
- [23] P. Murray-Rust, S. Motherwell, *Acta Cryst.*, B34 (1978) 2534–2546.
- [24] W.K. Olson, J.L. Sussman, *J. Am. Chem. Soc.*, 104 (1982) 270–278.
- [25] A.D. French, V. Tran, *Biopolymers*, 29 (1990) 1599–1611.
- [26] A.D. French, M.K. Dowd, P.J. Reilly, *J. Mol. Struct. (Theochem)*, 395–396 (1997) 271–287.
- [27] B.R. Leeftang, J.F.G. Vliegthart, L.M.J. Kroon-Batenburg, B.P. van Eijck, J. Kroon, *Carbohydr. Res.*, 230 (1992) 41–61.
- [28] J.R. Grigera, *J. Chem. Soc., Faraday Trans. 1*, 84 (1988) 2603–2608.